

Numerical study of electromagnetic wave propagation characteristics in collapsed building for rescue radar applications

Kyeol Kwon¹  | Dong-Kyoo Kim²  | Youngwoo Choi² | Jaehoon Cho¹ |
Kyung-Young Jung¹ 

¹Department of Electronics and Computer Engineering, Hanyang University, Seoul, Rep. of Korea.

²Hyper-connected Communication Research Laboratory, Electronics and Telecommunications Research Institute, Daejeon, Rep. of Korea.

Correspondence

Kyung-Young Jung, Department of Electronics and Computer Engineering, Hanyang University, Seoul, Rep. of Korea.

Email: kyjung3@hanyang.ac.kr

Since the Gyeongju earthquakes in 2016, there have been increased research interests in the areas of seismic design, building collapse, and rescue radar applications in Korea. Ground penetrating radar (GPR) is a nondestructive electromagnetic method that is used for underground surveys. To properly design ground penetrating radar that detects buried victims precisely, it is important to study electromagnetic wave propagation channel characteristics in advance. This work presents an electromagnetic propagation environment analysis of a trapped victim for GPR applications. In this study, we develop a realistic collapse model composed of layered reinforced concrete and a victim positioned horizontally. In addition, the effects of rebars and the distance between the radar antenna and target are investigated. The numerical analysis presents the electromagnetic wave propagation characteristics, including amplitude loss and phase difference, in the 450-MHz and 1,500-MHz frequency band, and it shows the electric field distribution in the environment.

KEYWORDS

collapse, electromagnetic analysis, finite-difference time domain method, ground penetrating radar, rescue radar

1 | INTRODUCTION

On September 12, 2016, the Republic of Korea experienced its largest ever earthquake since 1978, which is when the government began to monitor seismic activity. The earthquakes, which had a maximum M_L 5.8 and over 1,000 aftershocks occurred continuously on the south-eastern Korean peninsula, Gyeongju [1]. These earthquakes highlighted the fact that the Republic of Korea is no longer safe against earthquakes in spite of the fact that there has been low seismic activity in the Korean peninsula to date. The provincial government of North Gyeongsang announced that property damage from these strong earthquakes and the several hundred aftershocks in Gyeongju amount to \$20.8 million, including

some 4,900 shattered rooftops, cracked walls, and 32 injuries to humans [2]. As opposed to Japan, which has suffered from major earthquakes and tsunamis for a long time, much of the infrastructure in the Republic of Korea was not designed considering earthquake resistance. In the Republic of Korea, seismic design regulations were established in 1988, and thus buildings that were constructed before the development of earthquake-resistant designs are susceptible to lateral forces generated from earthquakes. Earthquake-resistant buildings currently account for 60% of apartments in the Republic of Korea; however, only 37% of apartments in Seoul, for a long time [3]. Besides earthquakes, sinkholes, poor construction, dilapidated facilities, and improper maintenance are reasons for the breakdown of old buildings.

Ground penetrating radar (GPR) is a very important tool for search and rescue operations after disasters such as earthquakes or floods [4]. In order to prevent damage due to the lack of location information of victims under debris, it is of great importance to accurately detect their exact locations. There are different non-destructive search and rescue methods, such as acoustic, seismic, and electromagnetic techniques [5–10]. As an electromagnetic method, GPR can be used in a variety of media, and has advantages such as instant data collection and high lateral resolution. However, the depth of penetration is limited, and depends on the building material, radar operating frequency, and radiated power. As the conductivity of building materials increases, the penetration depth decreases because the electromagnetic energy is more quickly dissipated, leading to a loss in signal strength at greater depths. Although higher frequencies do not penetrate as far as lower frequencies, they can give better resolution [11].

GPR detects buried objects by using information from the transmitted wave and the reflected wave from a target. It is very important to study electromagnetic wave channel characteristics of the collapse of buildings to enable the suitable design of GPR systems for rescue radars. In this work, an electromagnetic propagation environment is modeled based on the characteristics of existing old apartments in Seoul, Republic of Korea. The collapse model is composed of reinforced-concrete (RC) layers and the human body model. We investigate electromagnetic wave propagation characteristics in the collapse model, such as path attenuation, phase difference, and electric field distribution. In this numerical study, we employ the finite-difference time domain (FDTD) method because of its accuracy and robustness [12–15].

2 | METHODOLOGY

In GPR applications, collapsed buildings are extreme cases, and differ from ordinary archaeological environments. The electromagnetic wave energy decays in RC that is composed of a rebar lattice. In the higher frequency band, the penetration depth is shorter than that at the lower frequency band, but this can be advantageous for propagation through RC, and can provide higher resolution. In this work, we investigate electromagnetic wave propagation characteristics in a collapsed building both in the low- and high-frequency bands. Toward this purpose, we analyze the collapse model in both the 450-MHz and 1,500-MHz bands to determine how electromagnetic waves propagate in complex environments.

Before proceeding with realistic collapsed building structures, we first investigate a simple RC layered collapse model, as shown in Figure 1A. A GPR antenna is located above a five-layer-RC (1 m × 1 m × 0.125 m, 5 ea). The

rebar spacing is 50 mm, and the diameter of the rebar is 10 mm. The electrical properties of concrete were adopted from the ITU-R recommendation ($\epsilon_r = 5.31$, $\sigma = 0.03027$ S/m at 450 MHz and $\epsilon_r = 5.31$, $\sigma = 0.045265$ S/m at 1,500 MHz) [16]. The rebars in the design were set as perfect electric conductors (PEC). To analyze the propagating environment, a wide-band quasi horn antenna was used for the ground penetrating radar. The antenna is well-matched from 400 MHz to 2 GHz, and an input power of 1 V was delivered to the antenna port [17–19].

The time-averaged field intensity is depicted in Figures 1B and C for two collapse models at 450 MHz and 1,500 MHz, respectively. Compared to the collapse model without rebars, the field intensity exhibits more attenuation for the collapse model with rebars. This phenomenon holds for both the 450-MHz and 1,500-MHz bands. Note that the signal strength is proportional to the field intensity. As expected, electromagnetic fields are more focused for the higher band owing to the smaller wavelength relative to the

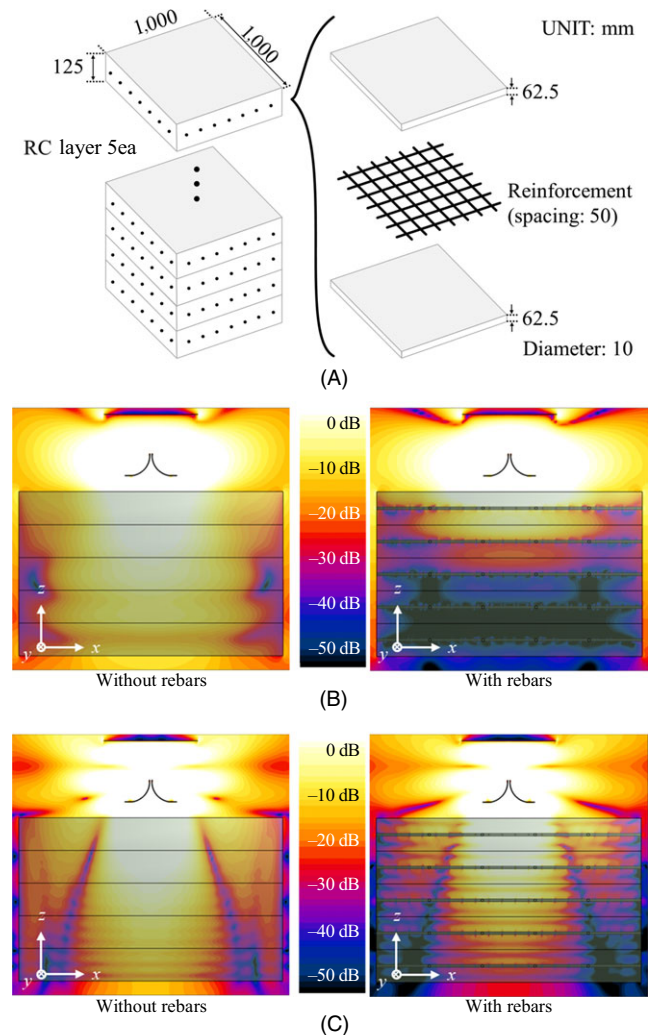


FIGURE 1 Time-averaged field intensity in RC layers: (A) RC layered collapse model, (B) field intensity at 450 MHz, and (C) field intensity at 1,500 MHz

lower band. It should be noted that a higher field intensity was observed for the 1,500-MHz band below the RC layers compared with the 450-MHz band. The penetration depth of the wave is generally proportional to the wavelength. However, in the collapse model with rebars, there are electromagnetic shielding effects that are due to the rebar lattices [20]. This implies that a suitable GPR frequency band depends on the complexity of the environment.

Figure 2 shows the path attenuation of the RC-layered collapse model. To determine the role of the rebar lattice, we performed a parametric study of the rebar spacing. The rebar spacing values that we adopted are 50 mm, 200 mm, and 400 mm, and these are represented as RC #1, RC #2, and RC #3, respectively. The observation point is 30 mm below the bottom plane of the collapse model. Using a concrete model as a reference level, the path attenuation of RC #1 is higher in the 450-MHz band than 1,500-MHz because of electromagnetic shielding effects. However, the path attenuation decreases as the rebar spacing increases in the 450-MHz band. Note that the path attenuation of RC #3 is even lower than that of the concrete model. Moreover, the path attenuation of RC #2 is lower than that of RC #3 in the 1,500-MHz band. These phenomena indicate that it is difficult to estimate accurate path attenuation owing to the resonance resulting from the rebar lattices [21]. Therefore, the margin of path attenuation is needed by considering the worst-case scenario in the design of GPR applications.

3 | NUMERICAL RESULTS

Next, we consider a collapsed building model that is based on the floor plan and reinforcement placing of existing apartment buildings constructed before the implementation

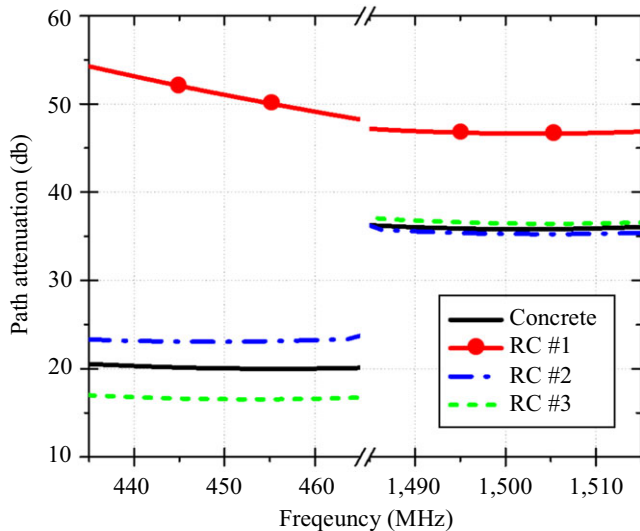


FIGURE 2 Path attenuation of RC-layered collapse model

of seismic design regulations in the Republic of Korea, as illustrated in Figure 3 [22]. To consider the worst case, layered RC ceilings were used for the debris of the collapse. The dimension of the environment is $2\text{ m} \times 2\text{ m} \times 2\text{ m}$. As mentioned previously, we employed geometrical parameters obtained from [22]. The thickness of the ceiling and the wall are 175 mm and 125 mm, respectively. The rebar spacing values of the top and bottom of the ceilings are 175 mm and 350 mm, respectively, and the rebar spacing of the walls is 250 mm. The diameter of the rebar is 10 mm. To consider the victim under collapse, a human-body model software developed by the IT'IS (Information Technologies in Society) foundation was adopted [23]. The model is a 34-year-old male lying on the floor of the collapse void. The electrical property of the human model used is that for dry skin ($\epsilon_r = 45.753$, $\sigma = 0.7088\text{ S/m}$

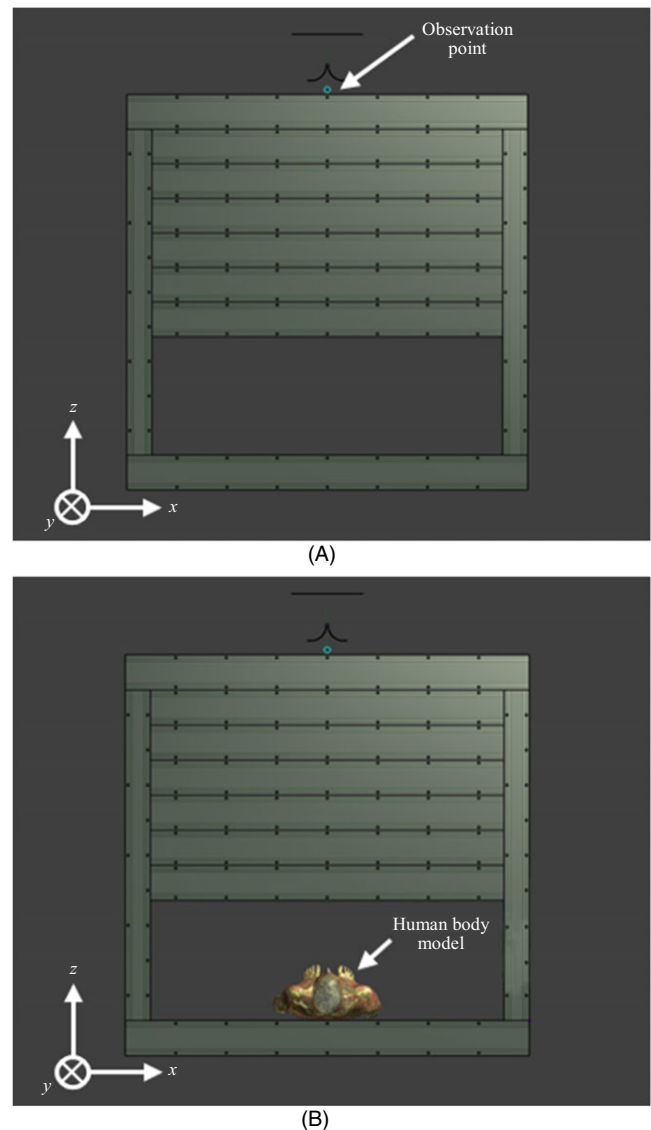


FIGURE 3 Collapsed building model: (A) model without victim and (B) model with a victim

at 450 MHz, and $\epsilon_r = 39.433$, $\sigma = 1.0716$ S/m at 1,500 MHz) [24]. Note that the distance from the center of the aperture of the GPR antenna and the top of the collapse model is 60 mm. The observation point is located 50 mm below the center of the antenna aperture. The distance between the antenna and the top of the chest of the human model is 1,591 mm.

In order to determine the reflected signal from the human body model, we simulated separately two collapsed building models (with a victim and without a victim). In other words, the electromagnetic wave at the observation point for the model with a victim (Figure 3B) is subtracted by the electromagnetic wave at the same point for the model without a victim (Figure 3A). Using this field extraction method, we can obtain the amplitude and phase information of the reflected wave due only to the presence of the victim.

In order to determine the effect of the RC thickness and the distance between the GPR antenna and a target, we modeled three cases. Figure 4A shows the case with a 7-ceilings and 1-bottom model (7C1B), which represents the worst case. For comparison with the case of Figure 4A, Figure 4B shows a 3-ceilings and 1-bottom model (3C1B), which has the same distance between the antenna and the target, but with fewer RC layers. Finally, the 3-ceilings and 5-bottoms model (3C5B) is depicted in Figure 4C. The last case has the same number of ceilings and overall structure size as the model shown in Figure 4B. However, the distance between the antenna and the target is shorter than in the previous cases.

Figure 5 illustrates the round-trip path attenuation of the collapse models shown in Figure 4. The path losses decrease as the number of RC layers decreases because the reflections and resonances that occur in RC layers are reduced. Moreover, as the distance between the antenna and the target increases, the path losses are increased. This information is required when setting the design parameters of GPR applications, such as the penetration depth, available input power, and link budget.

Next, we consider a realistic collapsed building model. The most common collapse types can be assumed as “lean-to” collapses, which involve a collapsed load-bearing ceiling and a void [25].

Figure 6 shows the time-averaged field intensity in the collapse model in the 450-MHz band. As the electromagnetic wave propagates through the collapse model without rebars, electromagnetic energy is dissipated owing to the lossy concrete. For the collapse model with rebars, electromagnetic energy is severely attenuated owing to both lossy concrete and conductor lattices, especially for the locations near the left and right walls. Compared to the collapse model without rebars, the time-averaged field intensity is more complex because of the multiple reflections of rebars.

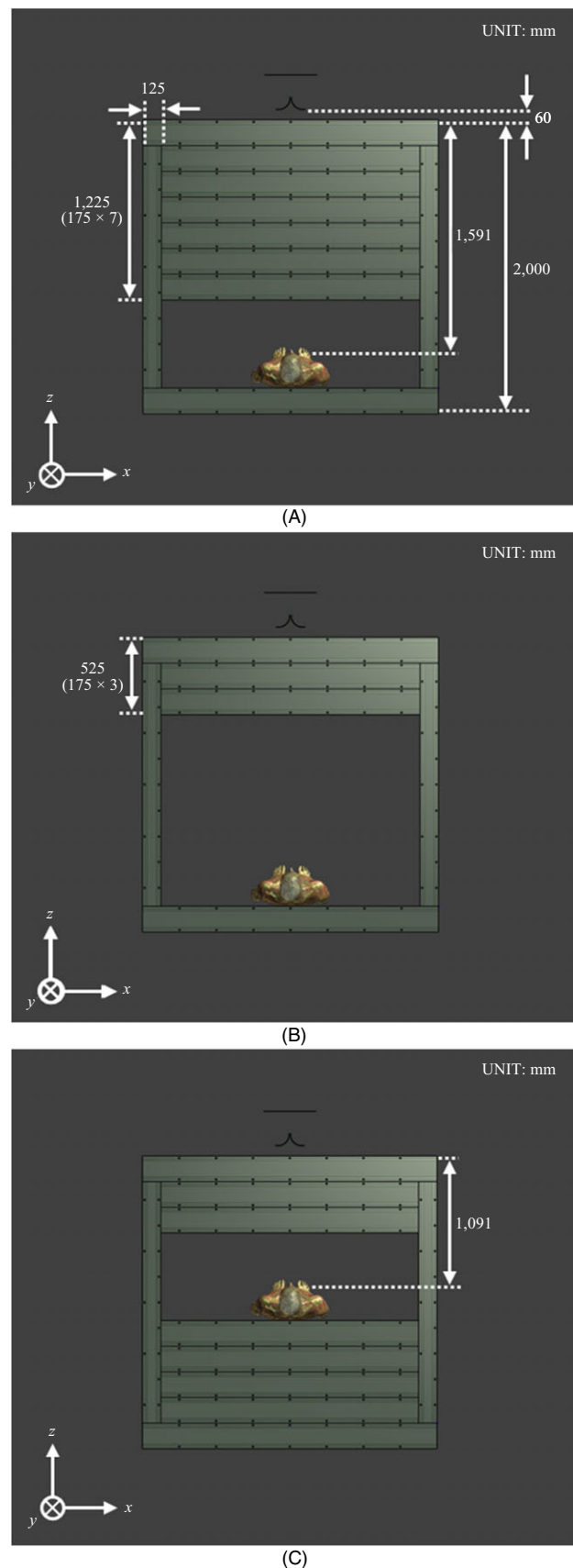


FIGURE 4 Simulation set-up for the collapsed building models: (A) 7-ceilings and 1-bottom model, (B) 3-ceilings and 1-bottom model, and (C) 3-ceilings and 5-bottoms model

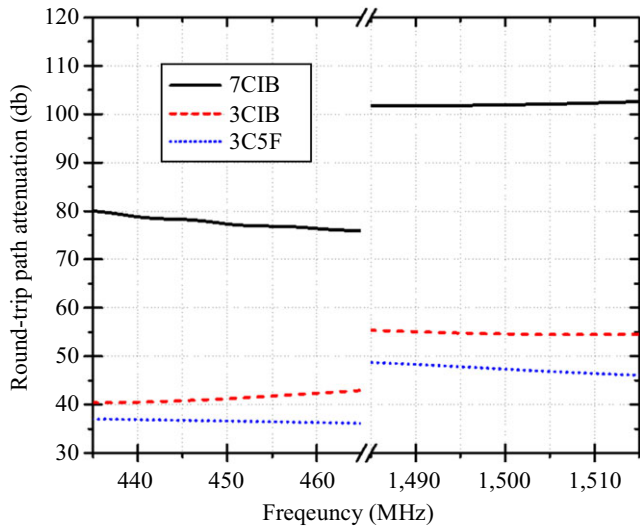


FIGURE 5 Round-trip path attenuation of collapsed building models

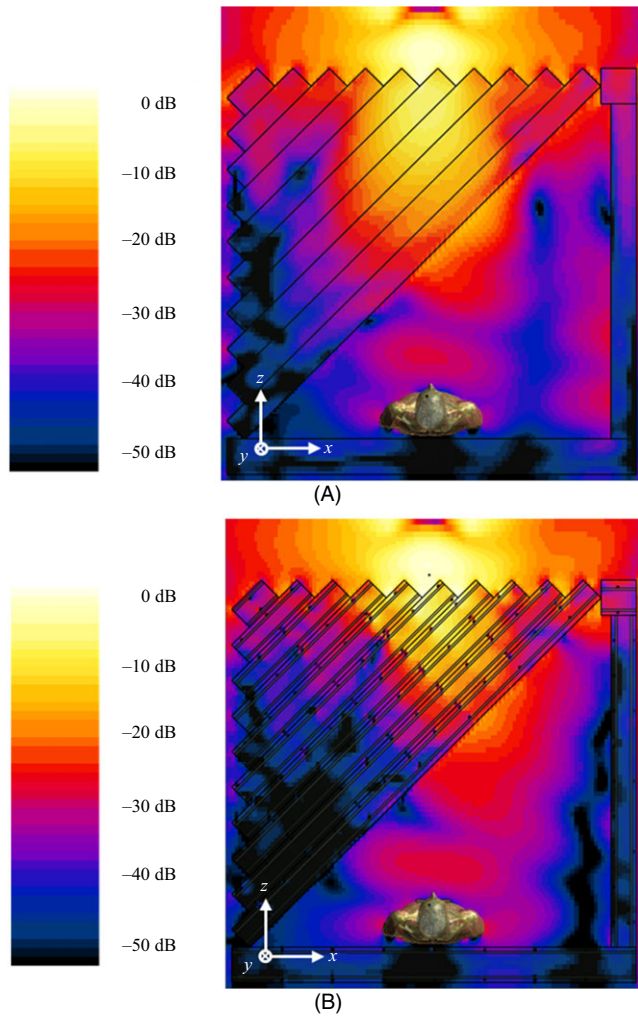


FIGURE 6 Time-averaged field intensity in the collapse model in 450-MHz band: (A) collapse model without rebar and (B) collapse model with rebar

To implement an enlarged thoracic cage of the victim during inhalation, a 10-mm-thick chest pad is placed on the chest of the body model (0.015λ at 450 MHz and 0.05λ at 1,500 MHz).

Figure 7 illustrates the phase differences between the exhalation and inhalation of the human body model. In the 450-MHz band, the phase difference between inhalation and exhalation is 1.74° . It is well known that the Doppler frequency can be estimated from the successive time series if the system phase noise level is low enough to distinguish the signal [26–29]. To detect a reflected signal clearly in the 450-MHz band, the phase-noise performance of the GPR system should be designed such that it is better than that of the higher band. By adopting the simulation data for micro Doppler, it is believed that a victim can be detected by his/her respiration [30, 31].

The time-averaged field intensity in the collapse model in the 1,500-MHz band is illustrated in Figure 8. As expected, the field distribution for the 1,500-MHz band is different from the corresponding distribution for the 450-MHz band. As depicted in Figures 8A and B, the electromagnetic energy is attenuated as it propagates through the layered structures. Note that the field intensity on the victim is lower than that of the lower frequency band. However, as shown in Figure 8B, the electromagnetic wave propagates further than expected through the rebar lattices. This phenomenon implies that the use of the GPR system in the 1,500-MHz band may be advantageous for complicated practical situations if a high input power is utilized for rescue radar applications that need high-resolution data.

Figure 9 shows the phase differences between exhalation and inhalation of the human body model. The phase difference between the inhalation and exhalation states is 6.44° in the 1,500-MHz band. Because the phase difference

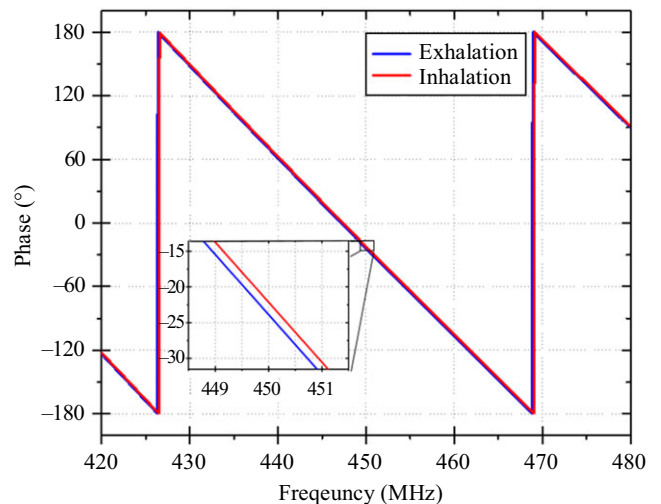


FIGURE 7 Phase differences between exhalation and inhalation of the human model at 450 MHz (inset diagram: $20 \times$ zoom window)

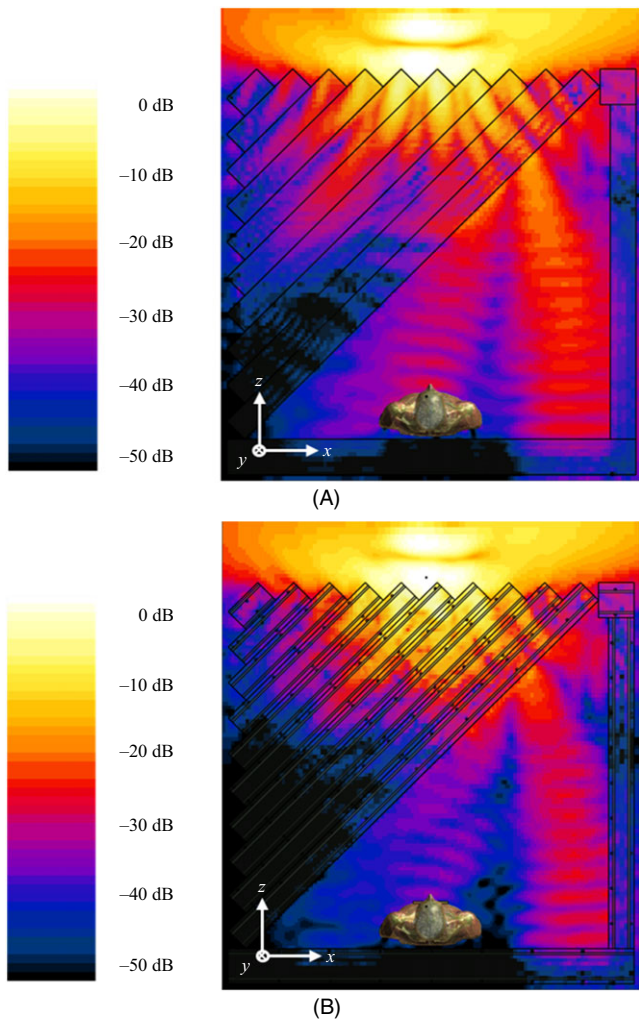


FIGURE 8 Time-averaged field intensity in the collapse model in the 1,500-MHz band: (a) collapse model without rebars and (b) collapse model with rebars

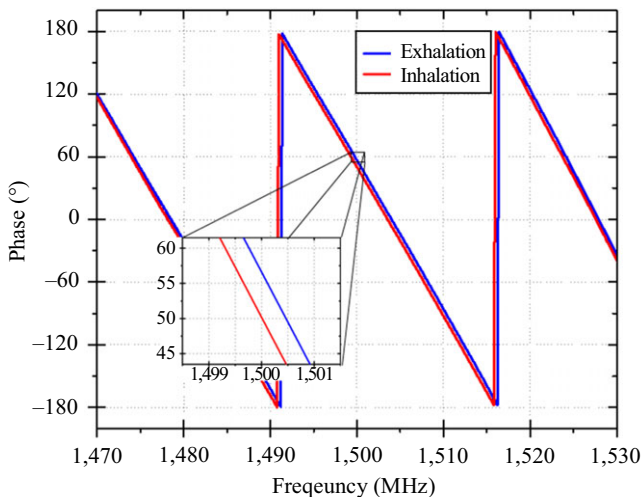


FIGURE 9 Phase differences between exhalation and inhalation of the human model at 1,500 MHz (inset diagram: 20 × zoom window)

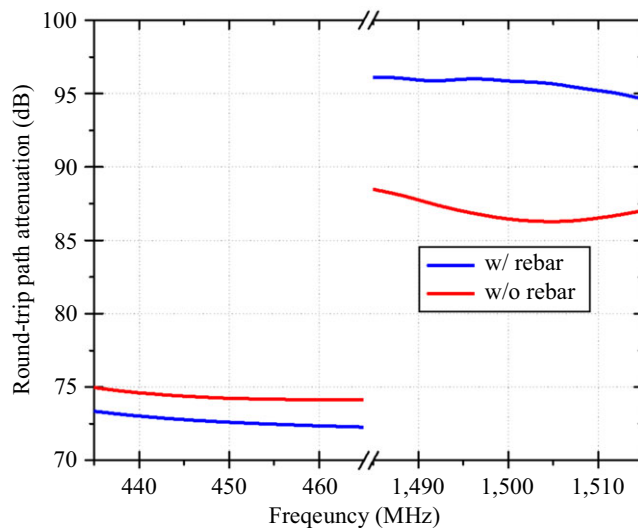


FIGURE 10 Round-trip path attenuation of the proposed collapse model

in the high-frequency band is greater than that in the low-frequency band, GPR radar can obtain higher-resolution data in the 1,500-MHz band compared with that in the 450-MHz band.

Figure 10 shows the round-trip path attenuation of the proposed collapse model. When the rebars exist, the path attenuations are 72.60 dB and 95.86 dB at 450 MHz and 1,500 MHz, respectively. If the debris is composed of concrete only, the path attenuations are 74.24 dB and 86.48 dB at 450 MHz and 1,500 MHz, respectively. As with the case involving the simple RC layered collapse, owing to resonances that result from the complicated metallic structure, the round-trip path attenuation for the collapse model with RC is lower than the model without RC in the 450-MHz band for this specific collapse model that is considered.

4 | CONCLUSION

In this paper, we presented an electromagnetic propagation environment analysis of buried victims for GPR applications. To determine the effects of rebars and the distance between the antenna and a target, we developed a realistic model that is based on the footprint of an existing old building in the Republic of Korea and the respiration of a victim model. Moreover, the field intensity and the path attenuation in a RC layered collapse model were investigated. In addition, we studied the differences in the electromagnetic wave propagation characteristics that are obtained for the low- and high-frequency bands. This feasibility study can provide design parameters for GPR systems, such as the path loss and link budget. By following the

numerical simulation procedure presented here, electromagnetic propagation analysis can be extended to various rescue operations such as flood and collapsed high-rise buildings.

ACKNOWLEDGEMENTS

This work was supported by the ICT R&D program of MSIP/IITP, Korea (B0117161001, Development of Original Fusion Technologies for Detecting Lung Cancer, Alzheimer's, and Buried People).

ORCID

Kyeol Kwon  <http://orcid.org/0000-0003-0149-2679>
 Dong-Kyoo Kim  <http://orcid.org/0000-0002-2360-1816>
 Kyung-Young Jung  <http://orcid.org/0000-0002-7960-3650>

REFERENCES

1. K. Kim et al., *The 12 September 2016 gyeongju earthquakes: 2. temporary seismic network for monitoring aftershocks*, *Geosci. J.* **20** (2016), no. 6, 753–757.
2. E. Choi, Y. Kim, and E. Chung, *Gyeongju quakes cost 23 billion won in damages*, Korea JoongAng Daily, 2016, available at <http://mengnews.joins.com/view.aspx?aId=3024096> (Accessed 24 Aug 2017).
3. Construction Policy Bureau, *Ministry of land, infrastructure, and transport*, Oct. 2013, available at <http://www.molit.go.kr>.
4. D. Daniels and J. David, *Ground penetrating radar. Encyclopedia of RF and microwave engineering*, ERA Technology, Surrey, UK, John Wiley & Sons, Inc., 2005.
5. A. Annan, *Electromagnetic principles of ground penetrating radar. Ground penetrating radar theory and applications*, Amsterdam, Netherlands, Elsevier, 2009, pp. 3–37.
6. A. Annan, *Ground penetrating radar, Near surface geophysics*, Society of Exploration Geophysicists, Mississauga, Canada, 2006, pp. 357–438.
7. Y. Lim and S. Nam, *Target-to-clutter ratio enhancement of images in through-the-wall radar using a radiation pattern-based delayed-sum algorithm*, *J. Electromagn. Eng. Sci.* **14** (2014), no. 4, 405–410.
8. G. Alsharahi et al., *Modelling and simulation resolution of ground-penetrating radar antennas*, *J. Electromagn. Eng. Sci.* **16** (2016), no. 3, 182–190.
9. D. Kim, B. Kim, and S. Nam, *A dual-band through-the-wall imaging radar receiver using a reconfigurable high-pass filter*, *J. Electromagn. Eng. Sci.* **16** (2016), no. 3, 164–168.
10. S. Yang and H. Ling, *Application of compressive sensing to two-dimensional radar imaging using a frequency-scanned microstrip leaky wave antenna*, *J. Electromagn. Eng. Sci.* **17** (2017), no. 3, 113–119.
11. L. Conyers and D. Goodman, *Ground-penetrating radar: An introduction for archaeologists*, AltaMira Press, Michigan, USA, 1997, pp. 149–194.
12. A. Taflove and S. Hagness, *Computational electrodynamics: The finite difference time domain method*, 3rd ed., Artech House, Norwood, MA, USA, 2005.
13. S. Ha et al., *FDTD dispersive modeling of human tissues based on quadratic complex rational function*, *IEEE Trans. Antennas Propag.* **61** (2013), no. 2, 996–999.
14. Sim4Life 2.2.1.873 by ZMT. available at www.zurichmedtech.com (Accessed 2017).
15. A. Lee et al., *Numerical implementation of representative mobile phone models for epidemiological studies*, *J. Electromagn. Eng. Sci.* **16** (2016), no. 2, 87–99.
16. ITU-R Rec. P. 2040, *Effects of building materials and structures on radio-wave propagation above about 100 MHz*, Sept. 2013.
17. G. Alsharahi et al., *Modelling and simulation resolution of ground penetrating radar antennas*, *J. Electromagn. Eng. Sci.* **16** (2016), no. 3, 182–190.
18. P. Duangtang, P. Mesawad, and R. Wongsan, *Creating a gain enhancement technique for a conical horn antenna by adding a wire medium structure at the aperture*, *J. Electromagn. Eng. Sci.* **16** (2016), no. 3, 134–142.
19. J. Han, S. Yoon, and J. Lee, *Miniaturization of SIW-based linearly polarized slot antennas for software-defined radar*, *J. Electromagn. Eng. Sci.* **16** (2016), no. 4, 248–253.
20. S. Celozzi, G. Lovat, and R. Araneo, *Electromagnetic shielding*, Wiley Encyclopedia of Electrical and Electronics Engineering, Hoboken, USA, 2007.
21. Z. Bihua et al., *Experimental investigation of EMP shielding effectiveness of reinforced-concrete cell model*, presented at the *Asia-Pacific Conf. Environ. Electromagn.*, Shanghai, China, May 7, 2000, pp. 296–300.
22. L. Chung, J. Lee, and T. Park, *Shaking table test for seismic performance evaluation of non-seismic designed wall-type apartment*, *J. Korea Concr. Inst.* **18** (2006), no. 6, 721–728.
23. ITIS Foundation, available at <http://www.itis.ethz.ch/> (Accessed 2017).
24. C. Gabriel, *Compilation of the dielectric properties of body tissues at RF and microwave frequencies*, Brooks Air Force Base, Texas, USA, Rep. N.AL/OE-TR- 1996-0037, June 1996.
25. R. Downey, *Types of collapse*, WNYF, 1st, Jan. 2001, pp. 10–11, available at <http://www.chief-raymond-downey.com/documents/wnyf/2001%20January%20-%20Types%20of%20Collapse.pdf>
26. E. Zaikov et al., *Detection of trapped people by UWB radar*, presented at the *German Microw. Conf.*, Hamburg-Harburg, Germany, Mar. 10–12, 2008, pp. 1–4.
27. R. Fletcher and J. Han, *Low-cost differential front-end for Doppler radar vital sign monitoring*, presented at the *2009 IEEE MTT-S Int. Microw. Symp. Digest*, Boston, MA, USA, June 7–12, 2009, pp. 1325–1328.
28. A. Droitcour, O. Boric-Lubecke, and G. Kovacs, *Signal-to-noise ratio in Doppler radar system for heart and respiratory rate measurements*, *IEEE Trans. Microw. Theory Tech.* **57** (2009), no. 10, 2498–2507.
29. J. Hall, *Respiration, Guyton and hall textbook of medical physiology*, Elsevier Health Sciences, Philadelphia, USA, 2015, pp. 497–560.
30. K. Robinette, T. Churchill, and J. McConville, *A comparison of male and female body sizes and proportions*, Wright-Patterson air force base, Ohio, USA, Aerospace Medical Research Laboratory, Tech. Rep. AMRL-TR-79-69, July 1979.

31. F. Adib et al., Smart homes that monitor breathing and heart rate, presented at the *Annu. ACM Conf. Human Factors Comput. Syst.*, Seoul, Rep. of Korea, Apr. 18–23, 2015, pp. 837–846.

AUTHOR BIOGRAPHIES



Kyeol Kwon received his BS degree in electronics engineering from Konkuk University, Seoul, Rep. of Korea, and his PhD degree in electronics and computer engineering from Hanyang University, Seoul, Rep. of Korea, in 2010 and 2018, respectively. Since April 2018, he has worked at Samsung Electronics, Rep. of Korea, where he is currently a senior researcher. His current research interests include computational electromagnetics, with focus on near-field communication, electromagnetic interference, and electromagnetic compatibility analysis.



Dong-Kyoo Kim received his PhD degree in electronics and computer engineering from Pohang University of Science and Technology, Rep. of Korea, in 2004. He was a visiting researcher at the Georgia Institute of Technology, Atlanta, USA, in 2004. Since 2005, he has worked at the Electronics and Telecommunications Research Institute, Daejeon, Rep. of Korea, as a senior researcher. His current research interests include ground/wall penetrating radar, vital signal sending radar, and other remote-sensing and imaging technologies, indoor localization technologies, wireless communication systems, and IoT sensor devices.



Youngwoo Choi received his BS and MS degrees in electronic engineering from Korea University, Seoul, Rep. of Korea, in 1998 and 2000, respectively. He has been a researcher since 2000, and is currently working as a senior researcher at the Electronics and Telecommunications Research Institute, Daejeon, Rep. of Korea.

His current research interests include penetration radar technologies, indoor positioning system-based RF technology, and RF/analog circuit design.



Jaehoon Cho received his BS degree in communication engineering from Daejin University, Pocheon, Rep. of Korea, and his MS and PhD degrees in electronics and computer engineering from Hanyang University, Seoul, Rep. of Korea, in 2004, 2006, and 2015, respectively. From 2015 to August 2016, he was a postdoctoral researcher at Hanyang University. Since September 2016, he has worked at Hanyang University, where he is currently a research professor. His current research interests include computational electromagnetics, with a focus on electromagnetic pulse, electromagnetic interference, and electromagnetic compatibility analysis.



Kyung-Young Jung received his BS and MS degrees in electrical engineering from Hanyang University, Seoul, Rep. of Korea, in 1996 and 1998, respectively and his PhD degree in electrical and computer engineering from The Ohio State University, Columbus, USA, in 2008. From 2008 to 2009, he was a postdoctoral researcher at The Ohio State University, and from 2009 to 2010, he was an assistant professor with the Department of Electrical and Computer Engineering, Ajou University, Suwon, Rep. of Korea. Since 2011, he has worked at Hanyang University, where he is now an associate professor in the Department of Electronic Engineering. He was a recipient of the Graduate Study Abroad Scholarship from the National Research Foundation of Korea, the Presidential Fellowship from The Ohio State University, the Best Teacher Award from Hanyang University, and the Outstanding Research Award from the Korean Institute of Electromagnetic Engineering Society. His current research interests include computational electromagnetics, bio electromagnetics, and nano electromagnetics.